ISBN: 978-3-95450-214-1 ISSN: 2673-5490 doi:10.18429/JACoW-IPAC2021-THXB02

BEAM ARRIVAL STABILITY AT THE EUROPEAN XFEL

M. K. Czwalinna†, J. Kral, B. Lautenschlager, J. Mueller, H. Schlarb, S. Schulz, B. Steffen
Deutsches Elektronen-Synchrotron, Hamburg, Germany
R. Boll, H. Kirkwood, J. Koliyadu, R. Letrun, J. Liu, F. Pallas, D. E. Rivas, T. Sato
European X-Ray Free-Electron Laser Facility GmbH, Schenefeld, Germany

Abstract

Free electron laser facilities, such as the European XFEL, make increasingly high demands on the temporal stability and uniformity of the electron bunches, as pump-probe experiments aim for timing stabilities of few femtoseconds residual jitter only. For a beam-based feedback control of the linear accelerator, electro-optical bunch arrival-time monitors are deployed, achieving a time resolution better than 3 fs. In a first attempt, we recently demonstrated a beam-based feedback system, reducing the arrival time jitter of the electron bunches to the 10 fs level with stable operation over hours. In this work, we are discussing first results from examining the facility-wide temporal stability at the European XFEL, with attention to the contributions of various sub-systems and on the different time scales.

INTRODUCTION

The free-electron laser facility European XFEL went into operation in 2017 [1] with a 1.5 km long linear accelerator reaching up to 17.5 GeV and driving up to 3 separate SASE beamlines.

This facility is operated in a 10 Hz burst mode, in which electron bunch-trains with up to 4.5 MHz repetition within the burst and up to 600 µs duration are accelerated using RF modules based on superconducting cavities. Despite their high quality and thus small bandwidth, the RF field during the 600 µs burst allows for a flexible tuning of RF amplitudes and phases in the defined flattop regions. The tuning range is tightly limited (<0.5% beam energy, few degrees of RF phase), but sufficient for tailoring the longitudinal phase space of the electron bunches to the needs of the 3 SASE beamlines. The electron bunches are distributed to the different undulator sections with a combination of slow flattop kickers and fast kicker systems, which can also remove individual bunches from the train to direct them to the dump beamline, thus facilitating a flexible configuration of user bunch numbers and repetition rates, compare Fig. 1. The experimental halls are located another 1.3 km from this switching yard. The length of the beam transport line from the source point of the FEL radiation to the interaction point of the actual experiment can amount to 1km length, including several optical components for beam redirection, focussing and shaping of spectral and transverse properties. A detailed description of photon diagnostics can be found for the example of SASE 1 beamline in [2].

Already due to the large dimensions of this facility the topic of stability is of tremendous importance. In the early operation phase, the focus was put to transverse effects only, like the electron beam orbit stabilisation with fast and slow feedbacks, as well as thoroughly monitoring and adjusting the photon beam pointing. With the increasing number of high-resolution, timing sensitive experiments for which the residual timing jitter between FEL pulses and pump-probe laser pulses is a critical or even limiting factor, the stability of longitudinal aspects of the beam are now brought into focus.

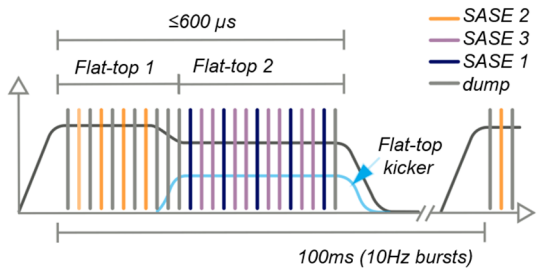

Figure 1: Bunch pattern layout of the European XFEL.

This concerns for example in the hard X-ray SASE1 beamline at FXE studies of ultra-fast dynamics of chemical/biochemical reactions, at the instruments for single particles, biomolecules (SPB) studies in the field of structural biology and at the soft X-ray beamline SASE3 the investigation of ultrafast processes with site-selectivity, with the instruments for soft X-ray coherent scattering/spectroscopy (SCS) and small quantum systems (SQS) [3]. For this type of experiments a low residual timing jitter between FEL photon pulses and pulses of external optical lasers is critical, especially where a post-sorting of data to achieve improved measurement resolution (e.g. described for data obtained at the FLASH facility [4]) is not applicable. For our studies presented here, we were concentrating on the instruments in SASE1 and SASE3 beamlines, since they are currently equipped with high-resolution photon arrival time monitors.

OPTICAL TIMING REFERENCE

An overview of the pulsed, laser-based synchronisation system at the European XFEL is given in [5]. The main laser oscillator (MLO) is locked with less than 5 fs rms in-loop jitter (bandwidth 10 Hz to 100 kHz) to the main RF oscillator (MO) of the facility. The RF reference signal is distributed to the acceleration sections via conventional RF cables, while the optical reference laser pulse train is distributed to the various end stations via individually length-stabilised fibre links (compare Fig. 2).

The client systems can be separated into three categories, which are shortly described in the following.

† marie.kristin.czwalinna@desy.de

ISBN: 978-3-95450-214-1 ISSN: 2673-5490 doi:10.18429/JACoW-IPAC2021-THXB02

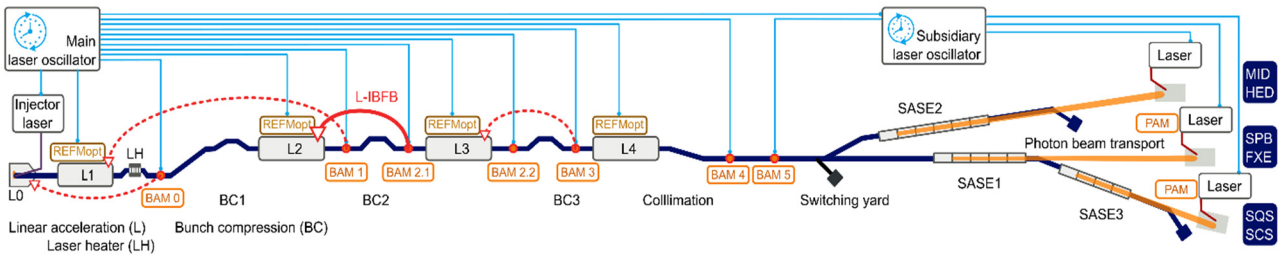

Figure 2: Schematic layout of the European XFEL facility, including several connections of the laser-based synchronisation system. The solid red line indicates the location of the established longitudinal intra-train feedback as introduced in this paper; the dashed red lines show the locations of the possible further intra-train feedback loops. In addition to the seven bunch arrival time monitors (BAMs), also the location of the photon arrival-time monitors (PAMs) at SPB and SQS instruments are indicated in this schematic.

RF- resynchronisation

The optical-to-RF reference modules (REFMOpt) detect and mitigate drifts of the distributed 1.3 GHz RF signal before it is further sub-distributed to the low-level RF (LLRF) controls of all connected RF modules. A detailed description of this device can be found in [6].

Optical Locking of External Laser Oscillators

The laser oscillator of the photo-injector is directly synchronised to the MLO signal. For locking the oscillators of all pump-probe laser systems to the optical reference, a second oscillator (SLO) in the experimental hall is used for a sub-distribution. The link in-between the MLO and SLO is nearly 3.5 km long which is equal to the length of the whole facility. Despite of its length, an in-loop integrated timing jitter of less than 2 fs has been reported for this length-stabilised fibre-link connection [5].

Pulse-resolved Measurement of Arrival-times

There are specific types of pulse-resolved arrival-time monitors which measure the timing of external systems with respect to the pulses of the optical reference:

- Laser pulse arrival-time monitor (LAM), which could be used closest possible to the experiment; such a system is currently under development.
- Photon pulse arrival-time monitor (PAM).
- Electron bunch arrival-time monitor (BAM).

All of these are suited for establishing feedback loops for a mitigation of timing drift and jitter at critical locations in the facility.

PHOTON ARRIVAL TIME MONITORS

The photon arrival-time monitors are using an electro-optical spectral decoding technique, in which a linearly chirped optical laser pulse (of the pump-probe laser system) spatially and temporally overlaps with the FEL pulse at the sample position.

The FEL pulse serves as pump in this case, changing the optical properties of the sample, such that the arrival time information is imprinted to the transmission modulation of the optical probe beam. The pure modulation signal has typically a step-like shape and thus can be fitted by an error function. Different spectral components of the chirped optical pulse arrive at the sample at different times, providing a direct mapping of wavelength to time. A detailed description can be found in [7]. The resolution limitation of this method is a combination of the fitting error (ca. 2.9 fs) and the time-to-pixel calibration error (ca. 1 fs) which results in an overall measurement uncertainty of only approximately 3 fs.

BUNCH ARRIVAL TIME MONITORS

The electron bunch arrival-time monitors are based on an electro-optical detection scheme. The electron bunch passing a broad-band (40 GHz) pick-up pair induces a voltage transient pulse which is guided together with a laser pulse of the optical reference through a Mach-Zehnder type electro-optical modulator [8]. The transmission of this modulator is normally set to 50% and the timing between both signals is adjusted such, that the laser pulse at perfect time overlap coincides with the zero-crossing of the voltage signal. Any timing drifts occurring between the electron bunches and the laser pulse train result in a non-zero voltage at time overlap, which changes the optical properties of the modulator substrate leading to a change in laser pulse transmission deviating from the 50% point. Thus, any timing change is translated into a transmission (or amplitude) modulation of the laser pulse. The sensitivity of this method is as good as 12 fs per % amplitude modulation. Using a suited timing scan and linear fit around the operation point, and taking the overall amplitude noise of the full signal chain into account, this yields a measurement uncertainty (single-shot) of approx. 2.8 fs.

STABILITY OF OPTICAL REFERENCE

For estimating the actual resolution of the arrival-time measurement, the correlation between two identical systems is used, in this example BAM3 (directly downstream of the last bunch compressor) and BAM4 (compare Fig. 2). They are separated by ca. 1.5 km straight section of the linac without any significant longitudinally dispersive element in between. Thus, the same temporal behaviour of the electron bunches is detected at these two locations.

ISBN: 978-3-95450-214-1 ISSN: 2673-5490 doi:10.18429/JACoW-IPAC2021-THXB02

BAM vs. BAM Correlation, Single-bunch

As shown in Fig. 3, the (single bunch) correlation width of BAM3 and BAM4 amounts to ca. 4.9 fs for 1 minute of data. The resolution σ_{BAM} of each individual monitor can be estimated from $\sigma_{\mathrm{BAM}} = \frac{1}{\sqrt{2}}\sigma_{\mathrm{noise}}$, thus equals 3.5 fs, which includes the residual noise of the optical reference system (i.e. the connection between MLO and BAM) and the limitations of the BAM system itself.

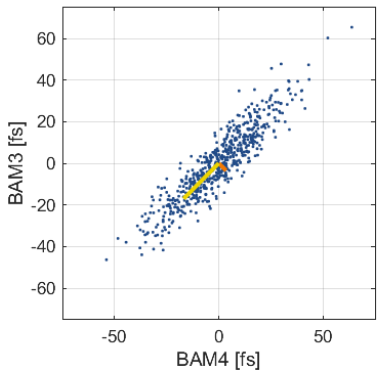

Figure 3: Single-bunch correlation plot of bunch No. 50 for 1 minute of data. The Pearsons' correlation coefficient is 0.92, the signal variation σ_{sig} has been 23 fs and the correlation width (or uncorrelated noise) σ_{noise} is 4.9 fs.

BAM vs. BAM Correlation, Train Mean-value

In order to estimate the low-frequency contribution to this obtained σ_{BAM} (or resolution) value which can be attributed to the residual noise of the optical reference, one can make use of the several hundreds of bunches at MHz repetition rate within the 10 Hz burst, by averaging over a sufficiently large number of bunches (in this case 334 bunches at 2.2 MHz rate). The correlation of the bunch-train mean values at BAM3 and BAM4 is shown in Fig. 4. The uncorrelated noise is reduced to σ_{noise} = 1.15 fs. This yields a contribution to the measurement uncertainty at each BAM of less than 1 fs ($\frac{1}{\sqrt{2}}\sigma_{\mathrm{noise}} = 0.8$ fs) in the range of 10 Hz up to approx. 5 kHz.

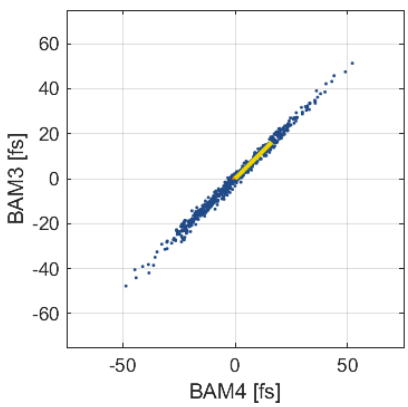

Figure 4: Correlation of the bunch-train mean values (from the same 1 minute of data set as in Fig. 3). The Pearsons' correlation coefficients is equal to 0.99, the correlation width (or uncorrelated noise) σ_{noise} is 1.15 fs.

BAM vs. PAM Correlation, Train Mean-value

Figure 5 shows the correlation of pulse-train mean arrival times, measured at the PAM in the SASE1 beamline (SPB instrument) and the BAM5 (located ca. 1.5 km upstream of the PAM). The correlation width σ_{noise} amounts to 12 fs, at measured signal variation σ_{sig} of 24 fs, equal for both monitors. Comparable values are obtained also at the SASE3 beamlines (SQS instrument).

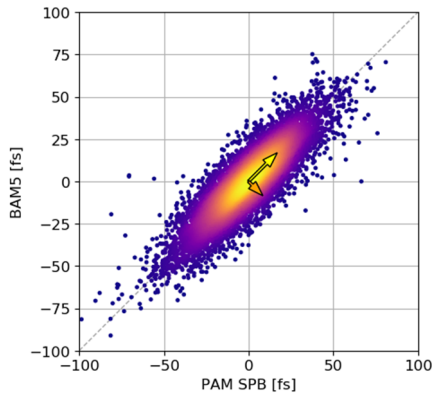

Figure 5: Correlation of the train mean-values of arrival times for the FEL photon pulses and the corresponding electron bunches, over a time window of 12 minutes. The Pearsons' correlation coefficient is 0.86 and the correlation width σ_{noise} is 12 fs.

This residual, short-term timing jitter between those two monitors is currently under investigation. Possible contributions to this noise are originating from the pump-probe laser synchronization, the laser amplifier chain, pulse compressor or frequency conversion.

ARRIVAL TIME STABILITY

As already reported in [1], measurements of the electron energy jitter give an upper limit for the rms relative energy jitter (rms) of 3×10^{-4} after the injector, 1.5×10^{-4} after BC1 and BC2 and 1×10^{-4} after the accelerator. Derived from a linear compression in the bunch compressors, the timing jitter after such a magnetic chicane in general dependents on three contributions:

- Incoming jitter $\Sigma_{t,i}^2$.
- Accelerator RF phase jitter $\sigma_{\phi_1}^2$.
- Relative RF amplitude noise $\frac{\sigma_{V_1}^2}{V_1}\sigma$.

Summarised in this equation:

$$\Sigma_{t,f}^2 = \left(\frac{R_{56}}{c_0}\right)^2 \cdot \frac{\sigma_{V_1}^2}{V_1} + \left(\frac{C-1}{C}\right)^2 \frac{\sigma_{\phi_1}^2}{\omega_{RF}^2} + \left(\frac{1}{C}\right)^2 \Sigma_{t,i}^2 \,. \quad (1)$$

The measured reduction of timing jitter by traversing the cascaded compression stages correspond with the design R56 [1]. As shown in Fig. 6, when looking onto the temporal behavior of the first bunch in the train, the 55 fs (rms) arrival-time jitter measured with BAM0 in the injector is stepwise reduced to a final value of ca. 17 fs (rms) at BAM3, 4 and 5 (redundant monitors).

ISBN: 978-3-95450-214-1 ISSN: 2673-5490 doi:10.18429/JACoW-IPAC2021-THXB02

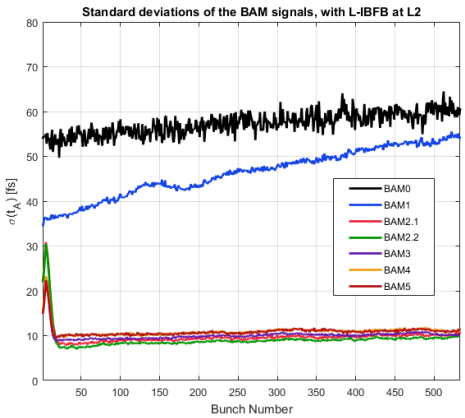

Figure 6: Arrival time jitter with active L-IBFB at L2 (using BAM2.1 as in-loop monitor). The first bunch in the train though shows the initial timing jitter evolution throughout the facility and is not affected by the feedback. The timing jitter of the following bunches reach a steady state after ca. 15 µs adaptation time. The L-IBFB acting upstream of BC2 reduces the initial (rms) timing jitter from around 23 fs to below 10 fs.

The actual arrival time jitter at final compression and final beam energy depends on the machine operation point (i.e. on the longitudinal phase space), but usual is between 15 fs and 25 fs (rms), for a nominal bunch charge of 250 pC, corresponding to a bunch length of less than 20 fs (rms) [1].

The centre-of-mass FEL pulse timing behaviour is in first order directly proportional to the centre-of-charge timing of the electron bunches, which is true in the case of a timing jitter comparable to or larger than the FEL pulse width. When looking onto time scales smaller than the FWHM of the FEL pulse, and at smaller numbers of radiation modes, the contribution from statistical fluctuations of the SASE process itself gains in importance.

The latest observation of the synchronization level at megahertz repetition rate had been published in 2020 [9].

With an optically synchronised pump-probe laser the residual jitter between laser pulses and FEL pulses was determined to 24 fs rms (± 12.4 fs), which fits to the here presented measurements.

In [9] also the difference between the pure RF lock and the optical lock of the pump-probe laser is discussed. The optical lock of the laser contributes to the jitter budget with as little as 6 fs rms, the optical link contribution is negligible, as shown in the above correlation measurements. Thus, the short-term jitter is in this case dominated by the FEL pulse jitter. Since this is the case, the residual jitter between FEL pulses and pump-probe laser pulses can be mitigated by applying beam-based feedbacks acting on the electron bunches.

BUNCH ARRIVAL-TIME INTRA-TRAIN FEEBACK

Longitudinal intra-train feedbacks which aim at reducing the burst to burst timing jitter can be established at locations in the accelerator where a translation from beam energy to arrival time takes place, i.e. in sections with a significant longitudinal dispersion, R56.

At the European XFEL, the multi-stage compression scheme offers three possible locations for such beam-based feedbacks (compare Fig. 2).

As described in the introduction, the specialty of the superconducting linac is the operation of long flattops which can be filled with up to 2700 bunches with a maximum repetition rate of 4.5 MHz. Since the selection of the bunches used for the generation of the FEL pules is done only after reaching the final bunch compression and final beam energy, all beam-based intra-train feedbacks in the linac can be operated at high bunch rates to achieve better stabilities.

The FEL pulse rate adjustment to lower values in the switching yard then does not affect the linac's operation point and performance. This argument applies to both, the transverse [10] and longitudinal intra-train feedbacks.

The perturbed bunches during the adaption time of the beam-based feedbacks can then as well be redirected to the dump beamline with a fast kicker, to make sure that the user bunches are located all in the stable, steady-state regions.

The method of a beam-based longitudinal intra-train feedback (L-IBFB) for mitigating the burst to burst arrival-time jitter, has initially been described in [11], but in the meantime has been adapted to the increased complexity of the LLRF controller for a better interplay of the different control loops acting on different time scales.

The general layout of the model-based RF controller design and the integration of the beam-based feedback part had already been introduced in [12]. The method uses an error combination and weighting of field-based and beam-based information for regulating the amplitude and phase of the field in an RF station prior to a bunch compressor using the arrival-time data measured at a downstream location.

The impact of the L-IBFB on the intra-train arrival time jitter is shown in Fig. 6. In this case, only the L-IBFB at L2 upstream of the second bunch compressor BC2 had been activated, using the arrival time data of BAM2.1.

The time required to reach steady-state depends on the overall system latency (signal transmission and processing) as well as on the system bandwidths (the quality factor of the superconducting RF cavities is about 3e6 which corresponds to a bandwidth of the field regulation of 50 kHz). The overall adaptation time needed is typically between 20 to 25 bunches, i.e. at the example of 1.1 MHz repetition rate, this amounts to ca. 20 µs for reaching a steady state.

As shown in Fig. 6, the incoming arrival time jitter at BAM2.1 (in-loop) and BAM2.2 (out-of-loop) can be reduced by more than factor 2, from initially 23 fs to about 9 fs using an L-IBFB. Also visible in Fig. 6 is that after the following chain of RF modules (in L3 prior to the last bunch compressor BC3) only a small amount of ca. 2 fs jitter is added.

ISBN: 978-3-95450-214-1 ISSN: 2673-5490 doi:10.18429/JACoW-IPAC2021-THXB02

The limitations of the L-IBFB are best visible in the frequency domain, as shown in Fig. 7. The displayed spectrum in the upper plot is the mean of the single spectra, calculated for each burst individually, using the mean free arrival time data (the same as used in Fig. 6).

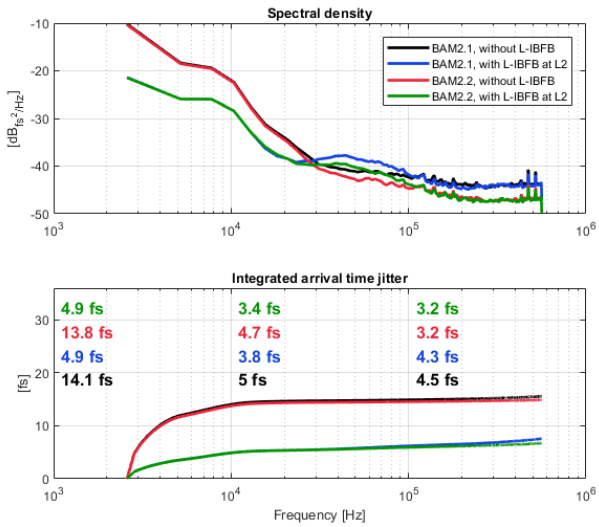

Figure 7: Spectral density and integrated timing jitter plots of the mean-free arrival time from 1minute duration, showing the comparison between the in-loop monitor (BAM2.1) and out-of-loop monitor (BAM2.2), for the two cases with and without L-IBFB (at L2) The main timing jitter reduction is achieved in the frequency range up to 25 kHz. The higher frequency range is dominated by the noise floor (or resolution) of the BAM system.

The upper and lower frequency limits of the spectrum are restricted by the frequency of the measured signal (1.1 MHz) and the number of available data points. The arrival time fluctuations are dominated by the frequencies up to 30 kHz (BAM2.1 and BAM2.2 without L-IBFB) and the floor level in the region above 100 kHz can be interpreted as BAM detector noise floor.

The four numbers in the lower part of Fig. 7 represent the contribution to the arrival time jitter per decade. The main effect of noise reduction is achieved up to 25 kHz bandwidth, whereas in the frequencies above this limit, noise is added again.

CONCLUSION

By the time of the measurements all required components of the synchronisation system and the relevant diagnostics (for electron and photon beams) had been fully commissioned and characterised. We demonstrated a good agreement between PAM and BAM measurements (for the mean bunch-train arrival time). Both monitor systems deliver reliable data and show a high-precision measurement with a resolution as good as 3 fs.

Using the BAM to BAM correlations, we could furthermore estimate the contribution of the optical reference system to the arrival time measurements to be less than 1 fs.

In a first attempt, an intra-train timing jitter reduction down to 10 fs has been demonstrated, using a beam-based, longitudinal intra-train feedback system at the RF station L2 prior to the second bunch compressor BC2.

OUTLOOK

With a combination of different feedback loops and optimization of the control parameters, we are expecting to further reduce the electron bunch jitter to below 5 fs on a reliable and reproducible basis.

The on-going investigation at SASE1 and SASE3 instruments will be extended to also SASE2 (the according PAM is in preparation) to identify the remaining drift and jitter contributions to the timing fluctuations between FEL pulses and pump-probe laser pulses.

Furthermore, the L-IBFB controls need a better automation to enable the set up by non-experts, and to improve the interoperability of slow (drift compensation) and fast (intra-train jitter reduction) corrections.

ACKNOWLEDGEMENTS

The authors acknowledge DESY Hamburg, Germany, the HGF and the European XFEL GmbH in Schenefeld, Germany, for the provision of XFEL beam time at the SPB/SFX instrument, and thank the instrument group and facility staff for their assistance.

REFERENCES

[1] W. Decking *et al.*, "A MHz-repetition-rate hard X-ray free-electron laser driven by a superconducting linear accelerator", *Nat. Photonics*, vol. 14, pp. 391-397, 2020. doi:10.1038/s41566-020-0607-z

[2] J. Grünert *et al.*, "X-ray photon diagnostics at the European XFEL", *J. Synchrotron Rad.*, vol. 26, pp. 1422-1431, 2019. doi:10.1107/S1600577519006611

[3] T. Tschentscher *et al.*, "Photon beam transport and scientific instruments at the European XFEL", *Appl. Sci.*, vol. 7, p. 592, 2017. doi:10.3390/app7060592

[4] E. Savelyev *et al.*, "Jitter-correction for IR/UV-XUV pump-probe experiments at the FLASH free-electron laser", *New J. Phys.*, vol. 19, p. 043009, 2017. doi:10.1088/1367-2630/aa652d

[5] S. Schulz *et al.*, "Few-Femtosecond Facility-Wide Synchronization of the European XFEL", in *Proc. FEL'19*, Hamburg, Germany, Aug. 2019, pp. 343-345. doi:10.18429/JACoW-FEL2019-WEP04

[6] T. Lamb *et al.*, "Femtosecond Laser-to-RF Synchronization and RF Reference Distribution at the European XFEL", in *Proc. FEL'19*, Hamburg, Germany, Aug. 2019, pp. 318-321. doi:10.18429/JACoW-FEL2019-WEB010

[7] H. J. Kirkwood *et al.*, "Initial observations of the femtosecond timing jitter at the European XFEL", *Opt. Lett.*, vol. 44, pp. 1650-1653, 2019. doi:10.1364/OL.44.001650

[8] A. Angelovski *et al.*, "Evaluation of the cone-shaped pickup performance for low charge sub-10 fs arrival-time measurements at free electron laser facilities", *Phys. Rev. ST Accel. Beams*, vol. 18, no. 1, p. 012801, 2015. doi:10.1103/PhysRevSTAB.18.012801

ISBN: 978-3-95450-214-1 ISSN: 2673-5490 doi:10.18429/JACoW-IPAC2021-THXB02

[9] T. Sato *et al*., "Femtosecond timing synchronization at megahertz repetition rates for an X-ray free-electron laser", *Optica*, vol. 7, no. 6, pp. 716-717, 2020. doi:10.1364/OPTICA.396728

[10] B. Keil *et al.,* "Design status of the European X-FEL transverse intra-train feedback", in *Proc IBIC'15*, Melbourne, Australia, Sep. 2015, paper TUPB064, pp. 492-493.

[11] F. Löhl *et al*., "Electron Bunch Timing with Femtosecond Precision in a Superconducting Free-Electron Laser", *Phys. Rev. Lett.*, vol. 104, no. 14, p. 144801, 2010. doi:10.1103/PhysRevLett.104.144801

[12] S. Pfeiffer *et al*., "Fast Feedback Strategies for Longitudinal Beam Stabilization", in *Proc. IPAC'12*, New Orleans, LA, USA, May 2012, paper MOOAA03, pp. 26–28.